# Sorption Studies of Propylene in Polypropylene. Diffusivity in Polymer Particles Formed by Different Polymerization Processes

**M. Patzlaff, A. Wittebrock, K.-H. Reichert**

*Institut für Chemie, Technische Universität Berlin, DE-10624 Berlin, Germany*

Received 12 April 2005; accepted 20 July 2005
DOI 10.1002/app.22723
Published online 9 February 2006 in Wiley InterScience (www.interscience.wiley.com).

**ABSTRACT:** Propylene was polymerized in gas phase and liquid phase by using a novel nonporous Ziegler–Natta-catalyst system. The polymer particles formed at different polymerization times were used for sorption measurements. In both cases it was found that the effective diffusion coefficient is increasing with increasing size of polymer particles and the effective diffusion coefficients of polymer particles formed by liquid-phase polymerization are larger than those of polymer particles produced by gas-phase polymerization. The effective diffusion coefficients of polymer particles are in the range of $2 \times 10^{-11}$ to $1.6 \times 10^{-10}$ $m^2/s$ with activation energies from 34 to 22 kJ/mol. The analyzed polymer particles have average diameters between 250 and 875 $\mu$m. The solubility of propylene in polypropylene particles can be described by the law of Henry at conditions studied. © 2006 Wiley Periodicals, Inc. J Appl Polym Sci 100: 2642–2648, 2006

**Key words:** polypropylene, Ziegler–Natta catalyst, sorption, diffusion coefficient

## INTRODUCTION

Sorption and desorption of low molecular weight components such as monomers, hydrogen, and diluents play an important role in gas-phase and slurry reactors. For kinetic modeling of olefin polymerization, solubility and diffusivity of monomer, hydrogen, and diluents in *insitu* formed polymer particles are needed. The solubility of penetrants in semicrystalline polymer is dependent on the properties of both the penetrant and the polymer. The sorption for sparingly soluble penetrants can be modeled by Henry's law because the sorbed amount is sufficiently small so that the polymer matrix does not undergo any swelling strain.[1] High soluble penetrants can swell and plasticize the polymer. This can even change the morphology of the polymer.[2] It is known that the morphology of a polymer particle is a replica of the original catalyst particle. Thus the morphology of catalyst plays an important role in the growth of polymer particles.

Sorption measurements can be performed in different ways. We used the gravimetric method with a magnetic suspension balance. This sorption method was also used by Garmatter,[3] Bartke,[4] by Schabel et al.,[5] Weickert et al.,[6] Gorval and Svejda,[7] Sato et al.,[8] and Kosek et al.[9] Further sorption methods are the inverse gas chromatography applied by Sliepcevich et al.[10] and the pressure decay method used by Sato et al.[11]

*Correspondence to:* M. Patzlaff (m.patzlaff@chem.tu-berlin.de).

Journal of Applied Polymer Science, Vol. 100, 2642–2648 (2006)


## EXPERIMENTAL

### Polymer sample preparation

Propylene (Merck, 3.5) without further purification was polymerized in gas and liquid phase with a novel nonporous Ziegler–Natta catalyst developed by BOREALIS Polymers Oy (Finland).[12–15] The catalyst contains 3.5 wt % Ti and 12.3 wt % Mg. All polymerizations were performed in a 100-mL stirred tank reactor (Premex, Switzerland). The catalyst was activated with a solution of triethylaluminum (TEA) as cocatalyst in pentane and dicyclopentylmethoxysilane (D-Donor) as an external donor. The activation of catalyst was conducted in an inert glovebox atmosphere. The external donor was first contacted with the solution of cocatalyst in pentane for 5 min at an Al/D ration of 10:1 to provide complexation. Dry catalyst (5 mg) was contacted in the reactor with half of the total amount of activation solution for 5 min. After removal of this solution the other half of activating solution was added. The molar ratio Al/Ti was 250:1. After connecting the reactor to the monomer pipeline and flushing with nitrogen for removal of air the monomer was added. For each polymerization process, propylene was used without further purifications. For gas-phase polymerization the monomer was fed through a mass-flowmeter into the reactor. For liquid-phase polymer-

**TABLE I**
**Polymer Samples Prepared for Sorption Measurements**

| Polymer sample | Polymerization process | Polymerization conditions | | |
|---|---|---|---|---|
| | | $T_{Polym.}$ (K) | $p_{Propylen}$ (bar) | $t_{Polym.}$ (h) |
| PP 122 | liquid phase | 343 | $p_{vapor}$ | 1 |
| PP 127 | liquid phase | 343 | $p_{vapor}$ | 1 |
| PP 128 | liquid phase | 343 | $p_{vapor}$ | 1 |
| PP 136 | gas phase | 328 | 5 | 4 |
| PP 138 | gas phase | 328 | 5 | 3 |
| PP 139 | gas phase | 343 | 5 | 2 |
| PP 145 | gas phase | 343 | 5 | 4 |
| PP 146 | gas phase | 343 | 5 | 5 |
| PP 150 | liquid phase | 343 | $p_{vapor}$ | 1 |
| PP 153 | liquid phase | 328 | $p_{vapor}$ | 2 |

ization a 50-mL steel cylinder was filled with liquid monomer. After weighing the cylinder the monomer was flushed with a nitrogen pressure of 15 bar into the reactor. The reactor was heated up to 328 or 343 K in several minutes. The stirrer speed was 290 revolutions/min. The polymerization time was varied between 60 and 300 min. After polymerization the reactor was cooled down quickly and residual monomer was removed. The polymer powder was sieved to obtain different fractions with average particle diameters ranging from 250 to 825 $\mu$m.

The polymer membranes were made from the same polymer product. A certain amount of polymer powder of a specific size fraction was placed in an aluminum form (with thickness of 400 or 1000 $\mu$m) and heated up to 453 K. The molten polymer was pressed in a press (Schwabenthan Polystat 200T) for 5 min at 20 bar and then for 5 min at 200 bar. Then the membranes were cooled down quickly from 453 to 313 K in 4 min.

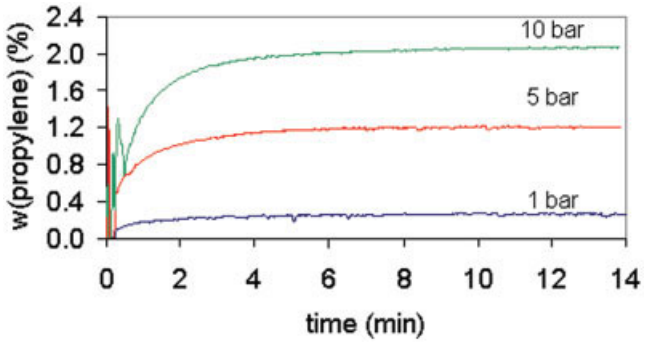


**Figure 1** It shows typical sorption curves at different propylene pressures. Weight fraction of propylene in polypropylene particles (PP 127; average diameter, 450 $\mu$m) at different pressures and 343K. [Color figure can be viewed in the online issue, which is available at www.interscience.wiley.com.]

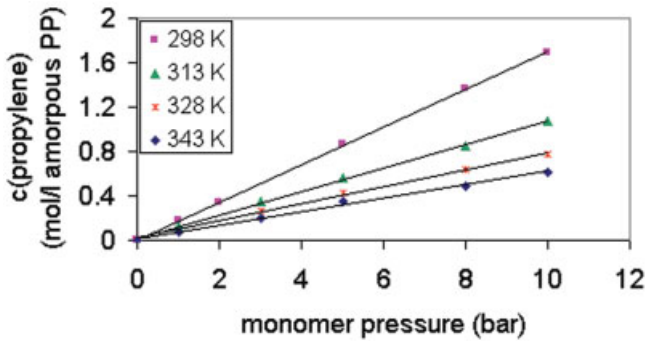


**Figure 2** Concentration of propylene in amorphous polypropylene of sample PP 150 as a function of pressure at different temperature. [Color figure can be viewed in the online issue, which is available at www.interscience.wiley.com.]

### Sorption measurements

Sorption measurements were performed in a magnetic suspension balance (Rubotherm Präzisionsmeβtechnik GmbH; Germany). A sample basket with the polymer inside was connected to an electronic microbalance (Mettler Toledo AT261 with an accuracy of 0.01 mg). The sample weight, gas temperature, and gas pressure were stored in a computer via a data acquisition unit. In the case of the increase of sample weight during measurements, the data were saved after considering the buoyancy influence as described in ref. 4.

For sorption measurements the sorption chamber was evacuated and filled with propylene. The temperature and pressure was varied between 298 and 353 K and 1–10 bar, respectively. The sorption pressure was reached after 10 s, at initial conditions.

## RESULTS

### Solubility of propylene in polypropylene

Table I gives an overview of used polymer particles for sorption measurements. Figure 1 shows typical sorption curves at different polypropylene pressures. Because of sorption of penetrants only into the amorphous part of the polymer, the crystallinity of polymer is needed for comparison of different polymer samples. The crystallinities of the polymer samples were

**TABLE II**
**Henry Coefficients for Propylene in Polypropylene (PP 150)**

| $T_{sorption}$ (K) | $k^*$ (this work; mol/$l^*$bar) | $k^*$ (Stern et al.; mol/$l^*$bar) |
|---|---|---|
| 343 | 0.06 | 0.07 |
| 328 | 0.08 | 0.09 |
| 313 | 0.11 | 0.12 |
| 298 | 0.17 | 0.17 |

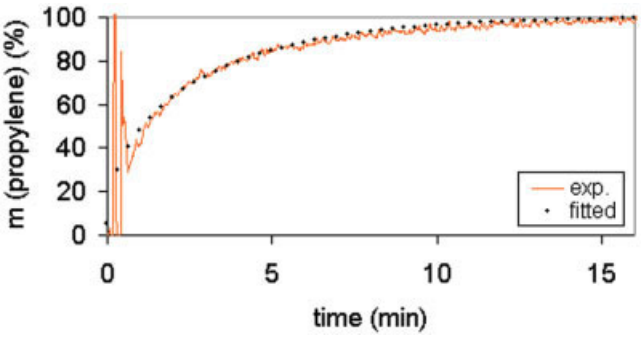


**Figure 3** Dynamic absorption characteristics of polymer particles (PP 128, 350 μm fraction) at 313 K and 5 bar propylene. [Color figure can be viewed in the online issue, which is available at www.interscience.wiley.com.]

analyzed using DSC (Perkin–Elmer, DSC-7). Thermophysical data needed to calculate the crystallinity, such as heat of fusion of a perfect crystal ($\Delta H$ = 209 J/g), were taken from ref. 16. The polymer particles showed crystallinities between 29 and 33 wt %. The polymer powder has a density of about 900 g/L and was estimated from sorption experiments described in ref. 4. The dependency of propylene concentration in the amorphous part of polypropylene at equilibrium on sorption pressure at different sorption temperatures is shown in Figure 2.

The concentration of absorbed monomer in polymer increases linearly with propylene pressure in measured pressure range. In agreement with results from Hutchinson and Ray 1, the sorption of propylene in polypropylene between 1 and 10 bar can be described by Henry's law. The Henry constants $k$ (mol/$l_{\text{Amorphous polymer}}$*bar) were compared with values, using eq. (1), proposed by Stern et al.[17]

$$\log(k^*) = -2.38 + 1.08(T_c/T)^2 \quad (1)$$

$T_C$ is the critical temperature of the penetrant ($T_C$ for propylene is 365 K[18]). Table II shows $k^*$ values from sorption measurements and values from eq. (1).

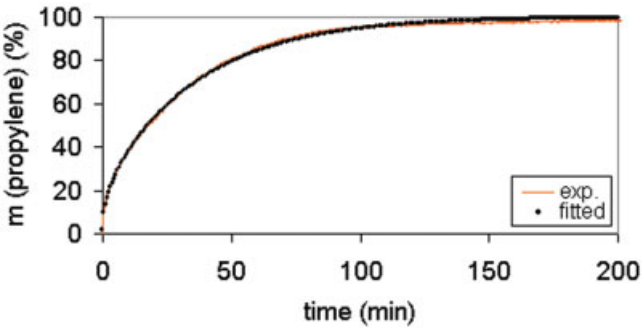


**Figure 4** Dynamic absorption characteristics of polymer membrane (PP 128, 1000 μm thickness) at 343 K and 5 bar propylene. [Color figure can be viewed in the online issue, which is available at www.interscience.wiley.com.]

**TABLE III**
**Reproducibility of Numerical Values of Diffusion Coefficient of Different Polypropylene Samples**

| Polymer sample | Particle size (μm) | $D_{\text{eff}} \times 10^{11}$ (m²/s) at 5 bar | $D_{\text{eff}} \times 10^{11}$ (m²/s) at 10 bar |
|---|---|---|---|
| PP 139 | 250 | 2.3 | 1.8 |
| PP 146 | 250 | 2.1 | 1.8 |
| PP 145 | 350 | 3.7 | 3.5 |
| PP 146 | 350 | 3.5 | 3.5 |

The $k^*$ values are in good agreement with theoretical values. The dependency of the Henry constant on temperature can be described by Arrhenius equation, applying with a sorption enthalpy of −17 kJ/mol.

## Diffusion coefficient of propylene in polypropylene

The diffusion of propylene in spherical polypropylene particles can be described by Fick's law. Based on ref. 19, solution of Fick's law for spherical particle yields:

$$\frac{m_M(t)}{m_{M,\text{Equi}}} = 1 - \frac{6}{\pi^2}\sum_{n=1}^{\infty}\frac{\exp(-D_{\text{eff}}n^2\pi^2 t/r^2_{\text{Particle}})}{n^2} \quad (2)$$

where $m_M$ is the mass of propylene absorbed; $m_{M,\text{Equi}}$, mass of propylene absorbed at equilibrium; $D_{\text{eff}}$, effective diffusion coefficient; $r$, average particle radius; and $t$ is the time of sorption.

The diffusion in a plane sheet can be described by the following equation:[19]

$$\frac{m_M(t)}{m_{M,\text{Equi}}} = 1 - \frac{8}{\pi^2}\sum_{n=0}^{\infty} \times \frac{\exp(-D_{\text{eff}}(2n+1)^2\pi^2 t/l^2_{\text{membrane}})}{(2n+1)^2} \quad (3)$$

where $l$ is the half thickness of the membrane.

**TABLE IV**
**Dependency of Diffusion Coefficient on Particle Diameter and Propylene Pressure at 343 K**

| Polymer sample | Particle size (μm) | $D_{\text{eff}} \times 10^{11}$ (m²/s) at 5 bar | $D_{\text{eff}} \times 10^{11}$ (m²/s) at 10 bar |
|---|---|---|---|
| PP 127 | 250 | 2.6 | 2.3 |
| (Liquid phase) | 450 | 5.3 | 5.0 |
| PP 153 | 350 | 4.1 | 4.0 |
| (Liquid phase) | 875 | 15.0 | 16.0 |
| PP 146 | 250 | 2.1 | 1.8 |
| (Gas phase) | 450 | 4.0 | 4.0 |

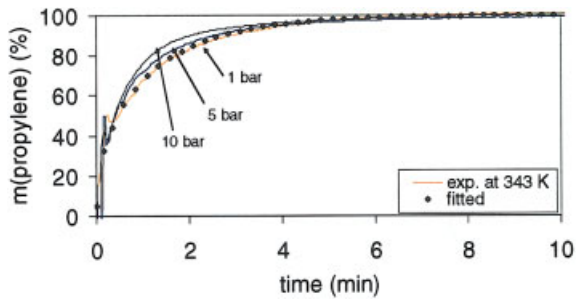


**Figure 5** Dynamic absorption characteristics of polymer particles (PP 150, 450 $\mu$m) at 343 K. [Color figure can be viewed in the online issue, which is available at www.interscience.wiley.com.]

The volume change of polymer samples during absorption of monomer was studied by videomicroscopy.[20] Swelling of polymer particles or membrane was not observed during the sorption processes and therefore not considered.

Depending on polymer samples (particle or membrane), eq. (2) or eq. (3) was fitted on sorption curves for determination of diffusion coefficients. Figure 3 shows a fitted sorption curve for polymer particles. An example for fitted sorption curves of propylene into a polymer membrane is given in Figure 4.

Equations (2) and (3) are able to describe the sorption curves quite well. Table III shows the numerical values of diffusion coefficients of different particle samples at different monomer pressures.

Polymer fractions that are polymerized at same conditions have same diffusion coefficients. Table IV shows values of effective diffusion coefficients for different polymer samples (gas- and liquid-phase product) with different particle diameters.

The diffusion coefficient is increasing with increasing particle size and is nearly independent with respect to propylene pressure at higher sorption temperature. The same effect was also observed by Sliepcevich et al.[10]. The dynamic sorption characteristics of polymer particles at 343 K for different sorption pressure are shown in Figure 5. At lower sorption temperature, the diffusion coefficient strongly depends on sorption pressure as shown in Figure 6. The corresponding diffusion coefficients are presented in Table V.

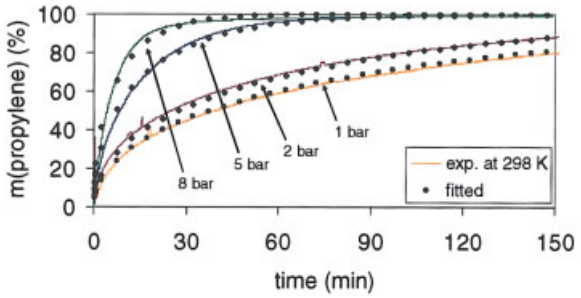


**Figure 6** Dynamic absorption characteristics of polymer particles (PP 150, 450 $\mu$m) at 298 K. [Color figure can be viewed in the online issue, which is available at www.interscience.wiley.com.]

**TABLE V**
**Dependency of Diffusion Coefficients on Sorption Pressure at Different Temperature (PP 150, 450 $\mu$m)**

| $p_{\text{Propylene}}$ (bar) | $D_{\text{eff}} \times 10^{11}$ (m$^2$/s) at 298 K | at 343 K |
|---|---|---|
| 1 | 0.1 | 11 |
| 2 | 0.2 | — |
| 5 | 0.7 | 12 |
| 8 | 1.4 | 13 |
| 10 | 1.6 | 14 |

The diffusion coefficient in polypropylene produced in gas-phase polymerization (PP 146) is smaller than the diffusion coefficient of a liquid-phase polymerization product (PP 127 and PP 153). The diffusion coefficients of polymer membranes are given in Table VI and compared with those of polymer particles of nearly same size.

The diffusion coefficients of polymer membranes are much smaller compared with those of polymer particles because the membranes have a compact structure. Diffusion coefficients for membranes of different thickness are given in Table VII. As expected, the diffusion coefficient does not depend on membrane thickness.

Sorption measurements were also made at different temperatures. In Figure 7, the temperature dependency of diffusion coefficient is shown in the range from 313 to 343 K.

The diffusion of low molecular weight components in solid polymers is an activated process and is described by the activation energy $E_D$ appearing in an Arrhenius-type equation :

$$D_{\text{eff}} = D_0 \cdot e^{\left(\frac{E_D}{RT}\right)} \tag{4}$$

where $D_0$ is a temperature independent frequency factor.

**TABLE VI**
**Comparison of Diffusion Coefficients of Polymer Particles and Membranes Measured at 343 K and 5-Bar Propylene**

| Polymer sample | Type of sample | $D_{\text{eff}} \times 10^{11}$ (m$^2$/s) |
|---|---|---|
| PP 138 | Particle (450 $\mu$m) | 4.5 |
| (Gas phase) | Membrane (400 $\mu$m) | 1.0 |
| PP 122 | Particle (625 $\mu$m) | 6.0 |
| (Liquid phase) | Membrane (400 $\mu$m) | 0.9 |

**TABLE VII**
**Diffusion Coefficients of Membranes of Different Thickness at 343 K and 5-Bar Propylene**

| Polymer sample for membrane preparation | Membrane thickness ($\mu$m) | $D_{eff} \times 10^{11}$ ($m^2/s$) |
|---|---|---|
| PP 122 (625 $\mu$m fraction) | 400 | 0.9 |
| PP 138 (250 $\mu$m fraction) | 400 | 1.0 |
| PP 122 (625 $\mu$m fraction) | 1000 | 1.0 |
| PP 128 (450 $\mu$m fraction) | 1000 | 1.1 |

**TABLE VIII**
**Influence of Particle Size on Activation Energy of Diffusion**

| Polymer sample | Particle size ($\mu$m) | $E_D$ (kJ/mol) |
|---|---|---|
| PP 128 | 350 | 28 ± 2 |
| (Liquid phase) | 625 | 22 ± 2 |
| PP 136 | 350 | 28 ± 2 |
| (Gas phase) | 450 | 22 ± 2 |
| PP 146 | 250 | 30 ± 2 |
| (Gas Phase) | 450 | 22 ± 2 |

The activation energy $E_D$ is a function of polymer molecular properties, such as the chain geometry or chain stiffness and the intermolecular forces.[21]

For polymer particles we estimated effective activation energies related to polymer properties and polymer morphology. The estimated activation energies of different polymer samples are shown in Table VIII. With increasing particle size the activation energy is decreasing.

The activation energy of 38 kJ/mol was determined for polymer membrane. This value is larger than the activation energies found for polymer particles and is due to the compact structure of the membrane. We do not further quantify the values of $E_D$. The diffusion in membrane can be described as molecular diffusion relating to polymer phase. So $E_D$ depends only from polymer molecular properties for example the distribution of crystalline regions in the polymer matrix because the crystalline parts in polymers constitute a diffusion resistance.

## Morphology of propylene particles

The particle size distributions of the polypropylene samples produced in liquid phase are narrower than those of polymer samples produced in gas phase (see Fig. 8).

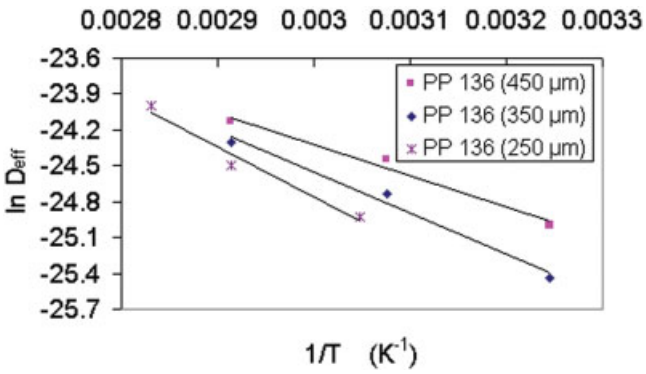


**Figure 7** Arrhenius plot of diffusion coefficient of polymer particles of different size. [Color figure can be viewed in the online issue, which is available at www.interscience.wiley.com.]

The morphology of polymer particles was studied using scanning electron microscopy (SEM; Hitachi S 2700).

Polymer particles are characterized by spherical shapes and can have compact or broken structures depending on polymerization method. Most of polymer particles produced in gas phase were observed to be more compact (Fig. 9, PP 146) than polymer particles produced in liquid phase (Fig. 9, PP 150).

Large polymer particles produced in gas phase or in liquid phase are observed to have much more broken structures than those of smaller ones. In case of small polymer particles from liquid-phase product a beginning of rupturing is visible (see Fig. 10).

SEM of cross-sectional cuts of polymer particles was used to study the internal structures of compact polymer particles. Polymer particles from gas-phase polymerization were observed to consist of compact polymer material. Only few particles were showing some small cracks and voids inside the polymer bulk (Fig. 11). Figure 12 shows details of the rupturing of particles produced in liquid phase.

The different effective diffusion coefficients of different polymer samples can be related to the different polymer particle morphologies observed. The high

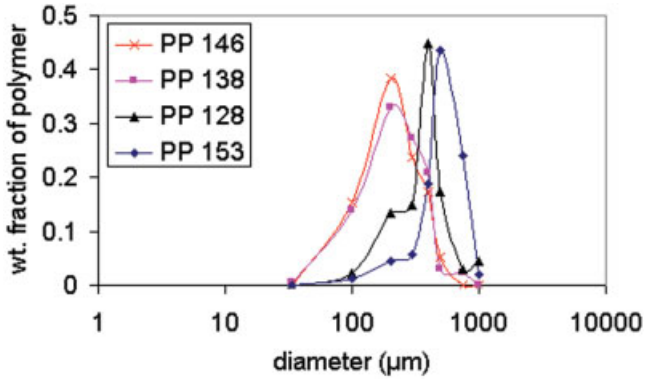


**Figure 8** Particle size distribution of polypropylene produced in gas phase (PP 138, PP 146) and in liquid phase (PP 128, PP 153) polymerization. [Color figure can be viewed in the online issue, which is available at www.interscience.wiley.com.]

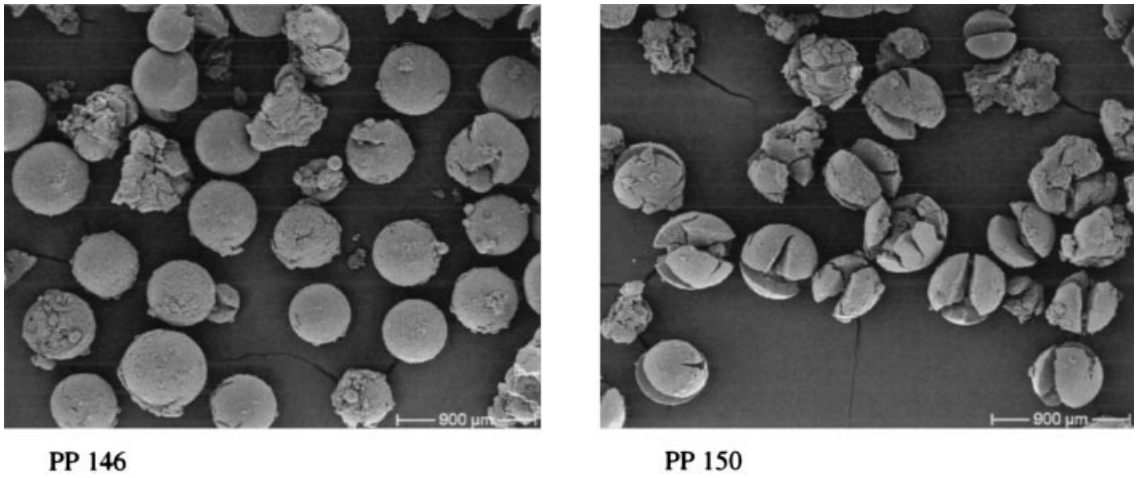


**Figure 9** SEM images of polymer particles produced in gas-phase (PP 146) and in liquid-phase (PP 150) polymerization.

values of effective diffusion coefficients observed in case of large polymer particles produced in liquid phase can by explained by their open structure due to the high degree of rupturing. The particle rupturing reduces the effective diffusion length in polymer material. Polymer particles of the same size produced in gas phase had smaller effective diffusion coefficients due to the more compact structure. In this case the effective diffusion length can be better correlated to the polymer particle radius. The significantly smaller effective diffusion coefficients determined for polymer membranes can be explained by their very dense structures, as observed with the SEM. The type of diffusion in polymer membrane can be described as molecular diffusion

## CONCLUSIONS

The increase of effective diffusion coefficients with increasing polymer particle size is probably due to the

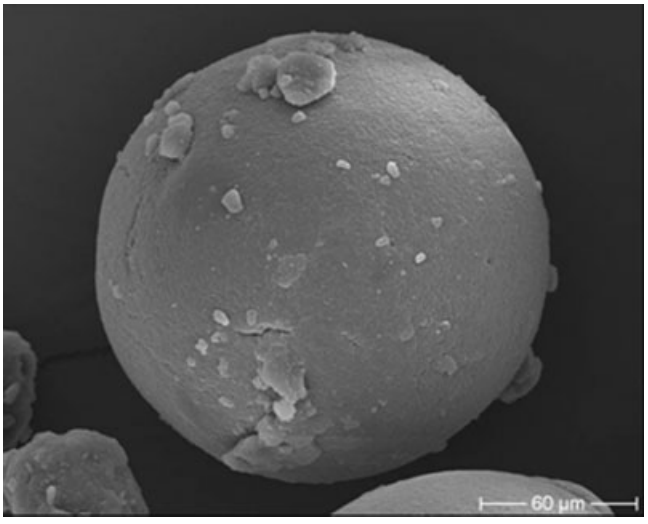


**Figure 10** SEM images of polymer particles produced in gas-phase (PP 146) and in liquid-phase (PP 150) polymerization.

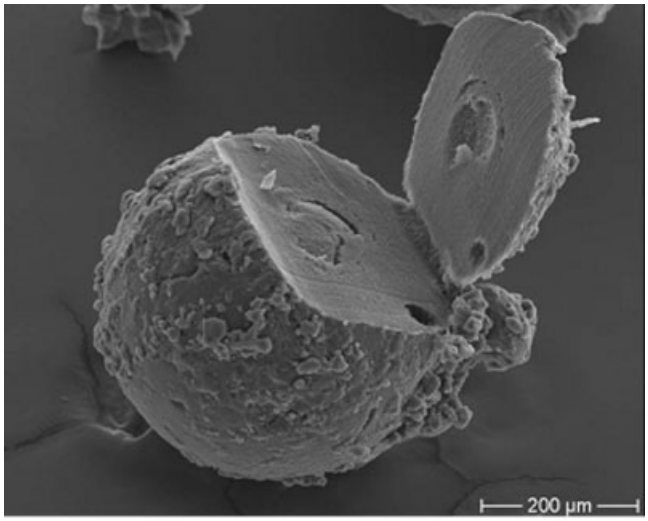


(a)

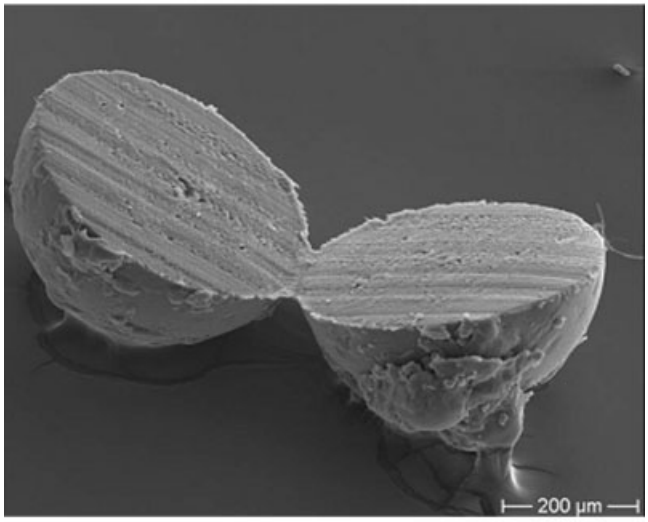


(b)

**Figure 11** Cross-sectional SEM images of polypropylene particles produced in gas-phase polymerization (PP 146).

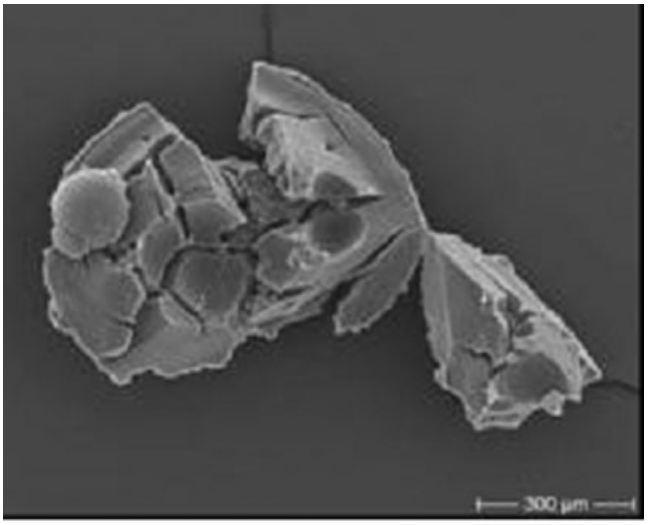


(a)

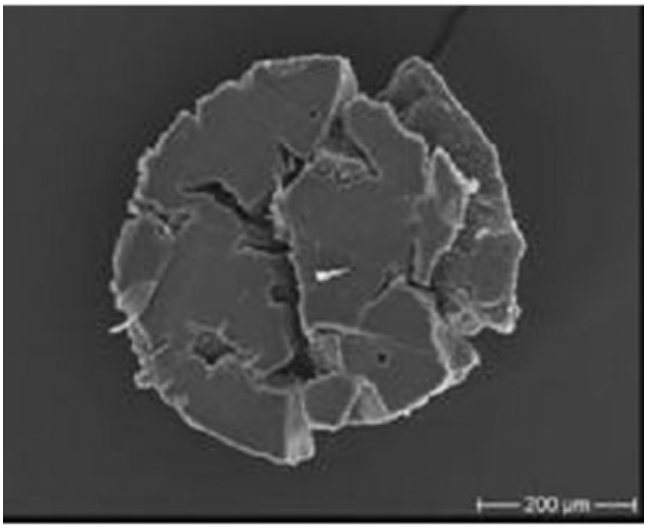


(b)

**Figure 12** Cross-sectional SEM images of cross section of polypropylene particles produced in liquid-phase polymerization (PP 150).

decrease of the effective length of diffusion within the polymer particle. This may be caused by the formation of voids or cracks in the polymer particles during the course of polymerization. Polymer particles formed by polymerization in liquid phase of monomer seem to be less compact than particles formed by polymerization in gas phase at same reaction conditions.

One reason may be the higher rate of polymerization in case of liquid pool polymerization leading to higher mechanical tension within the growing particles. Furthermore, differences in microstructure of polymer may also have to be considered.

Modeling of monomer transport in polymerizing particles therefore needs the consideration of changing diffusion coefficients during the course of polymerization.

The authors thank BOREALIS Polymers Oy (Finland) for supplying the catalyst and ZELMI-Institute of TU-Berlin for performing SEM pictures.

## References

1. Hutchinson, R. A.; Ray, W. H. J Appl Polym Sci 1990, 41, 51.
2. Stannet, V.; Yasuda, H. in Crystalline Olefin Polymers Part II; Raff, R. M. V.; Daak, K. W., Eds., Intersience Publishers: New York, 1964; p 131.
3. Garmatter, B. Ph.D. Dissertation, TU-Berlin, 1999.
4. Bartke, M. Ph.D. Dissertation, TU-Berlin 2002.
5. Schabel, W.; Mamaliga, I.; Kind, M. Chemie ingenieur Technik 2003, 75, S36.
6. Banat, Y.; Parasu Veera, U.; Weickert, G. in ECOREP II: European Conference on the Reaction Engineering of Polyolefins, Lyon, France 2002, 150.
7. Gorval, E. G.; Svejda, P.; Ind Eng Chem Res 2001, 40, 814.
8. Sato, Y.; Takikawa, T.; Sorakubo, A.; Takishima, S.; Masuoka, H.; Imaizumi, M. Ind Eng Chem Res 2000, 39, 4813.
9. Novak, A.; Kosek, J.; Snita, D.; Marek, M. in ECOREP II: European Conference on the Reaction Engineering of Polyolefins, Lyon, France, 2002, 119.
10. Sliepcevich, A.; Storti, G.; Morbidelli, M. J Appl Polym Sci 2000, 78, 464.
11. Sato, Y.; Yurugi, M.; Yamabiki, S.; Masuoka, H. J Appl Polym Sci 2001, 79, 1134.
12. Denifl, P.; Leinonen, T. Eur. Pat. 1273595A1 (2001).
13. Pöhler, H.; Denifl, P.; Leinonen, T.; Vestberg, T. Presented at MetCon 2003, Houston, TX, 2003.
14. Denifl, P.; Leinonen, T. Presented at EUPOC 2003, Milan, Italy, 2003.
15. Leinonen, T.; Denifl, P.; Vestberg, T. Presented at EUPOC 2003, Milan, Italy, 2003.
16. Quirk, R. P.; Alsamarraie, M. A. A. in Polymer Handbook, 3rd ed.; Brandrup, J., Immergut, E. H., Eds., Wiley: New York, 1989.
17. Stern, S. A.; Mullhaupt, J. T.; Gareis, P. J. AIChE J 1969, 15, 64.
18. VDI Wärmeatlas DC. Electronic version; Springer Verlag, 1998.
19. Crank, J. The Mathematics of Diffusion; Clarendon Press, Oxford, 1975.
20. Abboud, M.; Patzlaff, M.; Reichert, K. -H. in Dechema Monographien; Wiley-VCH: Weinheim, 2004; p 138. ISBN 3–527-10232–9.
21. Brandt, W. W. J Phys Chem 1959, 63, 1080.